

OPEN ACCESS

Dynamics of electron transfer at polar molecule–metal interfaces: the role of thermally activated tunnelling

To cite this article: J Stähler *et al* 2007 *New J. Phys.* **9** 394

View the [article online](#) for updates and enhancements.

You may also like

- [\(Invited\) Energetic Analysis of Interactions in Electron Transfer Complex Between Cytochrome C and Cytochrome C oxidase](#)
Koichiro Ishimori
- [Surface-induced intramolecular electron transfer in multi-centre redox metalloproteins: the di-haem protein cytochrome \$c_+\$ in homogeneous solution and at electrochemical surfaces](#)
Qijin Chi, Jingdong Zhang, Palle S Jensen *et al.*
- [Spatio-temporal dynamics of evapotranspiration on the Tibetan Plateau from 2000 to 2010](#)
Lulu Song, Qianlai Zhuang, Yunhe Yin *et al.*

Dynamics of electron transfer at polar molecule–metal interfaces: the role of thermally activated tunnelling

J Stähler, M Meyer, X Y Zhu¹, U Bovensiepen and M Wolf²

Freie Universität Berlin, Fachbereich Physik, Arnimallee 14,
14195 Berlin, Germany

E-mail: wolf@physik.fu-berlin.de

New Journal of Physics **9** (2007) 394

Received 4 June 2007

Published 31 October 2007

Online at <http://www.njp.org/>

doi:10.1088/1367-2630/9/10/394

Abstract. Heterogeneous electron transfer (ET) across interfaces is frequently discussed on the basis of Marcus theory taking into account the rearrangements of the solvent along a nuclear coordinate q . The ET process itself occurs via tunnelling through a barrier normal to the interface. The key point is not whether tunnelling occurs, but whether thermally activated solvent fluctuations initiate the tunnelling. Here, we discuss the role of thermally activated tunnelling in heterogeneous ET versus direct ET due to the strong electronic coupling to a metal substrate. As a model system, we investigate the ultrafast dynamics of ET at amorphous ice–metal interfaces (4–6 bilayers D₂O/Cu(111) and Ru(001), respectively) by time-resolved two-photon photoelectron spectroscopy. We find that the ET rate is *independent* of temperature within the first 500 fs after excitation, which demonstrates that for this system interfacial ET occurs in the strong-coupling limit and that thermally assisted tunnelling plays a negligible role.

¹ Present address: Department of Chemistry, University of Minnesota, Minneapolis, MN 55455, USA.

² Author to whom any correspondence should be addressed.

Contents

1. Introduction	2
2. Marcus theory for heterogeneous ET and the role of thermal activation	5
3. Experimental: time-resolved 2PPE spectroscopy	9
4. ET and solvation dynamics at the D₂O/metal interface	10
5. Summary and conclusions	12
Acknowledgments	12
References	13

1. Introduction

Electron transfer (ET)³ from a molecular donor to an acceptor state is one of the simplest conceivable reactions, as chemical bonds are neither formed nor broken. Such charge transfer reactions are of vital importance to a variety of processes in physics, chemistry and biology. For example, homogeneous ET is the primary step in photosynthesis [1, 2] and various chemical reactions [3, 4]. Heterogeneous ET at molecule–solid interfaces, on the other hand, plays an important role in technologically highly relevant fields. Examples are dye-sensitized solar (Grätzel) cells where light is converted into electrical energy by photoexcitation of adsorbed dye molecules and subsequent charge injection into the conduction band of a semiconductor substrate [5]. In addition, charge injection from a conducting electrode to a molecular system is of key relevance for the development of organic optoelectronic and nanoscale molecular devices [6, 7]. Furthermore, in the field of photochemistry at metal surfaces, transfer of photoexcited substrate electrons into unoccupied orbitals of adsorbed molecules provides a mechanism to induce chemical reactions by energy transfer to vibrational motion of the adsorbate [8, 9].

Different theoretical descriptions of charge transfer processes have been developed in the past [10]. Heterogeneous ET occurs along a real space ET coordinate, where tunnelling of the electron is mediated by wavefunction overlap between the donor and acceptor states. This picture has been frequently applied to describe the population decay of image potential states at metal surfaces [11] or the excitation process in surface photochemistry [12]. Depending on the degree of coupling between the electronic levels, a tunnelling barrier is assumed at the interface that determines the ET rate, whereby solvent fluctuations are assumed to play a negligible role [12]. An apparently different concept for charge transfer phenomena is the Marcus theory [13]–[15], which was originally developed to describe *homogeneous* ET (e.g. in solution) between two molecular levels. In this theory, charge transfer is rate-limited by nuclear motion of solvent molecules which arrange differently depending on the charge distribution of the solute (e.g. in donor–bridge–acceptor systems). The Marcus approach has also been extended to the heterogeneous ET problem and applied to charge transfer phenomena at molecule–semiconductor interfaces (e.g. dye-sensitized solar cells) [10, 16] and ET at organic–metal interfaces [17].

³ Although electron transfer is often also accompanied by electron transport, we do not use the latter term in the present work, as the electron transfer phenomena investigated here are mediated by tunneling and wave function overlap.

However, it should be noted that these seemingly different concepts for ET (Marcus theory versus tunnelling picture) are indeed complementary, as charge transfer in the presence of a solvent involves both nuclear rearrangement *and* tunnelling along the real space transfer coordinate. The tunnelling picture focuses on the pure ET process from the donor to the acceptor state along the real space coordinate, where the solvent influence is reflected in the shape of the potential barrier and minimum. Marcus theory in contrast mainly considers the influence of solvent fluctuations on the charge transfer rate, taking into account tunnelling along the real space coordinate by a transfer matrix element V_{DA} (see section 2). For a detailed understanding, identification of the actual *rate-determining step* is required: this could be either determined by the coupling between the electronic levels of donor and acceptor or by solvent rearrangement through thermal fluctuations which then is a prerequisite for tunnelling. Both pictures of charge transfer can be considered as a certain limit of a unifying concept, which involves both the electron and the nuclear (solvent) coordinates. This has been nicely explained by Truhlar and co-workers [18], who derived a theory for charge (proton) transfer taking into account both real space and solvent coordinates. Truhlar's concept uses a two-dimensional (2D) potential energy landscape that reflects the system's evolution from a donor to an acceptor state as a function of solvent *and* solute coordinate, respectively. The main idea is to treat the solvent and solute coordinate 'on a nearly equal footing' [18] and to understand the crossover between the solvent-controlled and the solvent-independent dynamics.

The corresponding 2D potential for *heterogeneous* ET from a solvated state (e.g. in a polar adsorbate layer [19]–[21]) to a metal electrode has to take into account the existence of a continuum of accepting states in the metal substrate and their delocalized nature. Figure 1 depicts a schematic contour plot of such a potential energy landscape of the solvated electron (donor state) and the lowest unoccupied (acceptor) states of the metal as a function of lattice distortion q (vertical axis) and ET coordinate z (bottom axis). The grey-shaded area corresponds to the metal and the white background to the adsorbate layers. As discussed in more detail below (see section 2), cuts through the 2D potential surface along either the ET coordinate z or the solvent coordinate q result in the electron potential energy along z for a fixed solvent distortion (figure 1(b))⁴ [23] or in the Marcus parabolas for the donor (V_D) and acceptor (V_A) states (figure 1(c)), respectively. The horizontal and vertical dashed lines indicate the corresponding cuts. However, it should be noted that this extension of Truhlar's concept to a 2D potential for heterogeneous ET is just schematic in order to illustrate the connection between the solvent motion and the electron tunnelling.

In this paper, we discuss the role of thermally activated tunnelling in heterogeneous ET at a metal surface. The key question is not whether tunnelling occurs, but whether thermally activated solvent fluctuations lead to instantaneous reduction of the tunnelling barrier and thus mediate the tunnelling rate. On the other hand, for sufficiently strong wavefunction overlap of the excess electron with unoccupied metal states, direct transfer without changes of the solvent configuration will dominate. In this work, we study the ultrafast electron solvation dynamics at amorphous ice–metal interfaces (several bilayers (BL) of D_2O adsorbed on Cu(111) and Ru(001)) using femtosecond time-resolved two-photon photoemission (2PPE) spectroscopy [22, 23]. Depending on the degree of coupling between the solvated excess electron in ice and the electronic states in the metal, different limits could be applicable for the description of the

⁴ The potentials shown in panel (b) are not single particle potentials and therefore differ from the commonly used image potential.

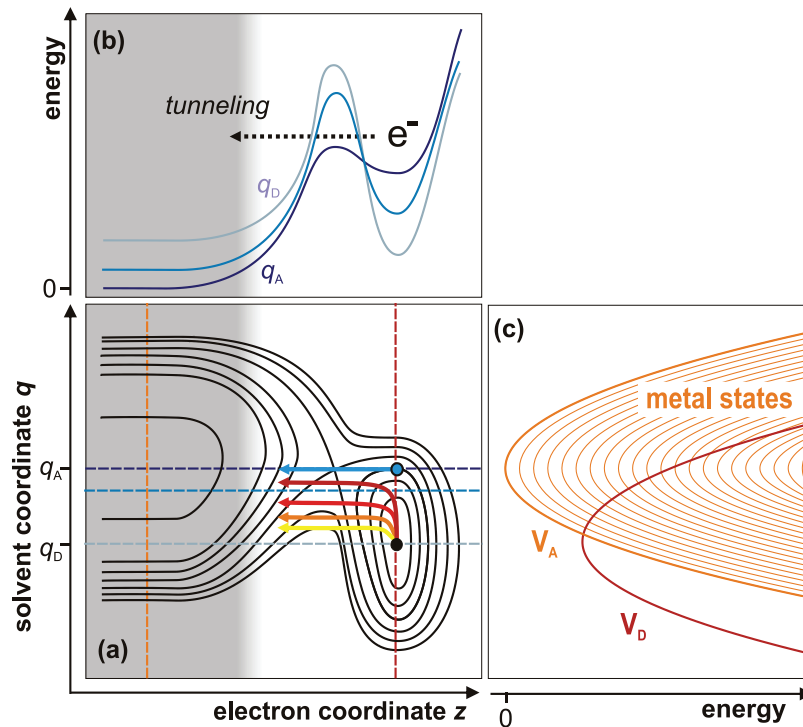


Figure 1. 2D model for ET at a metal surface: (a) the 2D potential energy surface of the electron–metal/solvent system for the donating polar adsorbate and the energetically lowest unoccupied (accepting) metal state along the real space coordinate z and the solvent coordinate q . Arrows illustrate direct ET due to strong electronic coupling (blue) and due to thermally assisted tunnelling (yellow to red, see section 2). (b) Horizontal cuts give the potential along the electron coordinate for a fixed lattice distortion. (c) Marcus parabolas of the solvated electron and the lowest unoccupied metal state (thick curves). The continuum of unoccupied acceptor states above V_A is illustrated by the thinner orange lines.

ET process. We discuss which coordinate, z or q , is most relevant for the charge transfer process at amorphous ice–metal interfaces. To do so, understanding of the influence of temperature on the ET rate is necessary as a thermally activated solvent rearrangement may facilitate the transfer process.

In section 2, the temperature dependence of the classical Marcus approach will be discussed. It will be shown that—depending on the free energy of the charge transfer reaction—heterogeneous ET in the weak-coupling limit can either be temperature-dependent or -independent. However, this theory of non-adiabatic ET is based on the assumption that the solvated electron is thermally equilibrated with its surroundings when charge transfer occurs. We show that adaptation of this description to the case of a photoinjected hot (i.e. non-thermalized) excess electron en route to localization as, for example, at ice–metal interfaces, results in an unambiguous temperature dependence of ET. Subsequently, the temperature-independent charge transfer occurring in the strong coupling limit will be discussed, showing that temperature-dependent experiments are a reliable probe for the character of charge

transfer. After a brief description of 2PPE spectroscopy (section 3), temperature-dependent measurements of the ET dynamics at amorphous ice–metal interfaces will be presented in section 4. The results allow for the determination of the rate-limiting step for charge transfer, i.e. solvent fluctuation or coupling strength. We find for amorphous D₂O/metal interfaces that the dynamics of ET directly after photoinjection is *not* thermally activated, which shows that ET at the investigated ice–metal interfaces occurs in the strong coupling limit.

2. Marcus theory for heterogeneous ET and the role of thermal activation

In the following, we discuss the role of thermally activated tunnelling in ET to a metal substrate using Marcus theory. Originally, Marcus developed his charge transfer theory for *homogeneous* transfer within a solvent, i.e. for the ET from one distinct molecular state to another [13]–[15]. The main challenge was to find a simple description for this multi-dimensional problem of donor, acceptor and the abundance of solvent molecules. In his classical theory, Marcus assumed that the motions of the solvent molecules occur within linear response limits, i.e. the displacements are so small that the assumption of a harmonic potential is applicable [24]. However, the infinite number of possible solvent configurations would lead to an enormously complex multi-dimensional potential energy surface. The black parabolas in figure 2(a) are slices through this potential energy landscape along a generalized solvent coordinate, assuming a fixed distance of donor and acceptor.

These potentials, V_D and V_A for donor and acceptor, respectively, are plotted as a function of the collective solvent coordinate q . This coordinate describes changes in the molecular configuration of the solvent. The potential minima at q_D and q_A correspond to the fully equilibrated species of donor and acceptor. At q_t , fluctuations of the solvent bring these two levels in resonance; this transition state region is often termed the adiabatic crossing point. Depending on the coupling strength V_{DA} between the two states, an avoided crossing of the potential occurs (see further below). In this *strong coupling limit*, charge transfer occurs adiabatically: if the system passes the ‘intersection’ by fluctuations, it will remain at the lowest potential. If there were *no* coupling between the levels, charge transfer would not occur at all. Considering very *weak coupling* between the donor and acceptor, fluctuations across q_t would make the system traverse to the upper potential surface and back [25]; in this case ET occurs with the probability

$$k_{\text{homo}} = \frac{2\pi}{\hbar} \langle V_{DA} \rangle^2 \text{FC}, \quad (1)$$

where V_{DA} is the coupling matrix element between the donor and acceptor level and FC is a thermally averaged Franck–Condon factor that describes the influence of temperature on the charge transfer rate by a Boltzmann distribution of the vibronic levels in the harmonic (parabolic) potential. The ET probability is thereby determined by the nuclear potential barrier ΔE_{equi} , which is the energy difference between the intersection at q_t and the donor potential minimum at q_D (cf figure 2(a), left). It depends on the reorganization energy λ and the free energy of the reaction ΔG^0 .

Extension of this model to the *heterogeneous* problem, i.e. the transfer from a distinct molecular state to a metal (electrode) offering a continuum of unoccupied states above the Fermi level E_F , requires a continuum of accepting states as illustrated by the manifold of grey curves in figure 2(a) [7, 10]. The energetically lowest level corresponds to the lowest unoccupied states

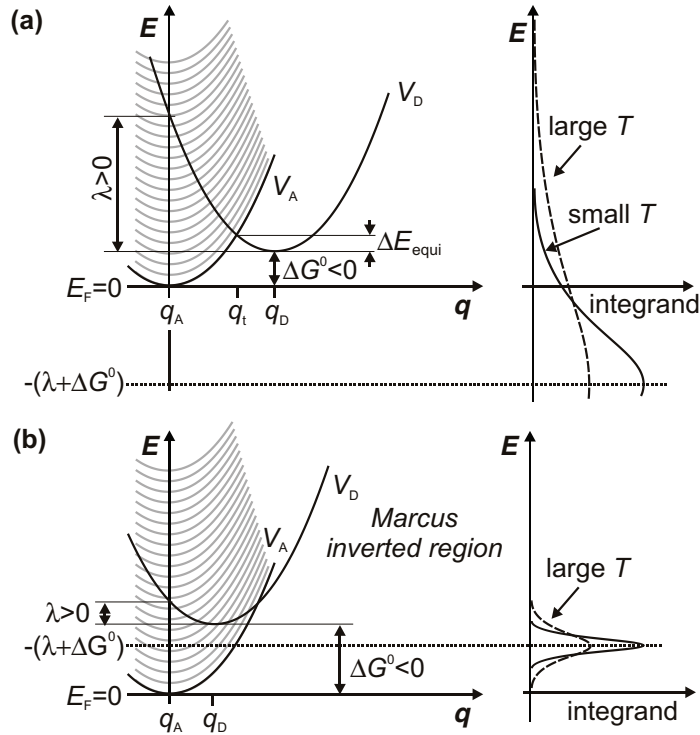


Figure 2. Marcus curves for heterogeneous ET from a molecular donor state V_D to a continuum of accepting substrate states (grey curves). (a) For $\lambda + \Delta G^0 > 0$ the charge transfer rate can be temperature-dependent, as the Gaussian distribution (right) is cut by the Fermi function according to equation (2). (b) In the inverted region, i.e. $\lambda + \Delta G^0 < 0$, ET is temperature-independent for sufficiently large $|\Delta G^0|$, as the Fermi function in equation (2) does not cut the Gaussian distribution considerably (right).

of the metal close to E_F , here denoted as V_A . The transfer rate from the donor state V_D to V_A exactly follows equation (1). However, transfer to the energetically higher lying states in the metal also contributes to the transfer rate. Thus, consideration of the varying energy difference between the respective potential minima is required. Integration of the resulting rate constants weighted by the Fermi–Dirac distribution $f(E)$ around E_F and the metal’s DOS $\rho(E)$ leads to the total rate of heterogeneous ET [10]:

$$k_{\text{hetero}} = \int_{-\infty}^{\infty} \frac{2\pi}{\hbar} \langle V_{DA} \rangle^2 (1 - f(E)) \rho(E) \left(\frac{1}{4\pi\lambda k_B T} \right)^{1/2} \exp \left\{ -\frac{[E + (\lambda + \Delta G^0)]^2}{4\lambda k_B T} \right\} dE. \quad (2)$$

The activation energy $\Delta E_{\text{equi}}^*(E) = (E + \lambda + \Delta G^0)^2/4\lambda$ for charge transfer results in a Gaussian distribution of transfer rates. For constant coupling V_{DA} and density of states $\rho(E)$ equation (2) can become temperature-dependent if $(\lambda + \Delta G^0) > 0$, i.e. the minimum of V_D lies below the intersection with V_A (cf figure 2(a)). ET requires thermal activation to overcome $\Delta E_{\text{equi}}^*(E)$, or, in other words, the Gaussian distribution in equation (2) is cut by the Fermi function (cf figure 2(a), right) maintaining the temperature dependence of equation (2) after

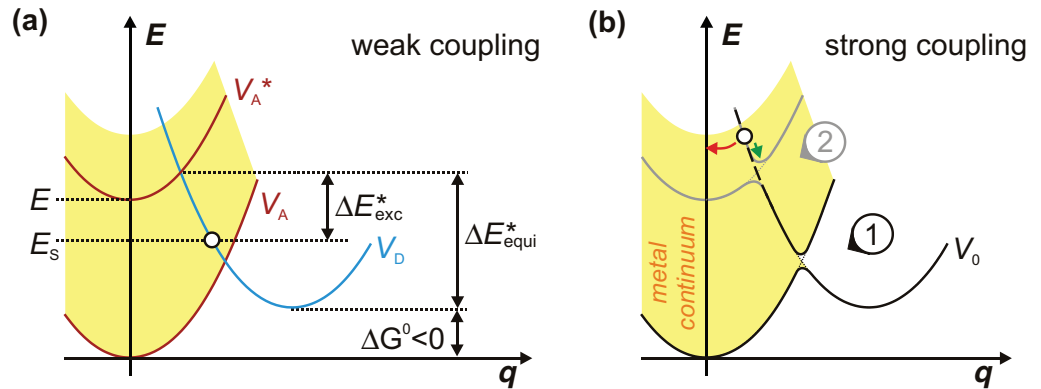


Figure 3. Heterogeneous ET of just photoinjected, excited electrons to the continuum of metal states (orange area). (a) Weak coupling limit: the nuclear barrier ΔE_{exc}^* is reduced by $E_S + \Delta G^0$ introducing an additional temperature dependence of the transfer rate. (b) Strong coupling limit: black curves (1) illustrate the level splitting for homogeneous ET. Due to the continuum of accepting metal states avoided crossings occurs at any energy, but (because of varying V_{DA}) the degree of splitting must not be similar (2). The green and red arrows illustrate the competition of ET and solvation.

integration. If $(\lambda + \Delta G^0) < 0$ the donor parabola V_D is in the inverted region (cf figure 2(b)). This means that V_D is intersected by acceptor levels down to its minimum and non-activated charge transfer can occur at any $q < q_D$, regardless of the Boltzmann distribution of donor states. If the Gaussian's width $(4\lambda k_B T)^{1/2}$ is sufficiently small ($|\Delta G^0|$ sufficiently large), the distribution is not considerably cut by the Fermi function (cf figure 2(b), right). This leads to a temperature *independence* of ET, as both temperature-dependent factors in equation (2) are cancelled by integration.

Note, that the above described approach of weak electronic coupling is based on the assumption of a thermally equilibrated system in the donor state [10]. This means that the process of electron solvation (i.e. equilibration with the solvent) has to occur on a much faster timescale than the ET. Such a Boltzmann distribution of molecular modes is not necessarily established for hot electrons in molecular adlayers on metal surfaces directly after photoinjection, as the transfer occurs here on fs-timescales. For these systems, ET and solvation compete with each other [23] and a thermally equilibrated solvated electron distribution around the potential minimum cannot be assumed. Figure 3(a) illustrates ET of a nascent excess electron en route to localization due to solvation that has not reached the potential minimum of V_D . The energy barrier ΔE_{exc}^* for charge transfer to the exemplary metal state V_A^* for the non-equilibrium hot electron is smaller than that of the equilibrated electron ΔE_{equi}^* by $E_S + \Delta G^0$. This reduction adds an additional exponential factor in the transfer rate integral in equation (2):

$$k(E_S) \propto \int \frac{2\pi}{\hbar} \langle V_{DA} \rangle^2 (1 - f(E)) \rho(E) \left(\frac{1}{T}\right)^{1/2} \times \exp\left(\frac{E_S + \Delta G^0}{k_B T}\right) \exp\left\{-\frac{[E + (\lambda + \Delta G^0)]^2}{4\lambda k_B T}\right\} dE. \quad (3)$$

The term $E_S + \Delta G^0$ is always positive and becomes zero when the solvated electron is fully equilibrated. It introduces a temperature dependence of the transfer rate, which is *not* cancelled out in contrast to the case of the equilibrium description in the Marcus inverted region (figure 2(b)). In conclusion, in this picture, where constant V_{DA} and $\rho(E)$ are assumed, charge transfer is *always* temperature-dependent as long as the system has not reached the V_D minimum ($E_S + \Delta G^0 > 0$).

In fact, the above assumption of energy-independent V_{DA} and ρ is questionable, since a solvated electron dynamically *changes* its degree of confinement, as shown in a previous publication [19]. Thus, the assumption of a constant coupling matrix element V_{DA} certainly does not hold true. Instead, the coupling decreases significantly upon solvation (see [23]). Equation (2) becomes independent of temperature only if the integrand remains a Gaussian with an energy-independent amplitude proportional to $T^{-1/2}$. Thus, *any* energy dependence of the pre-factors in equation (2) that varies the Gaussian distribution results in a temperature dependence of the transfer rate. A change of $V_{DA}(E)$ due to dynamic solvation can therefore, cause a temperature dependence of the system, even if it is in the Marcus inverted region and in thermal equilibrium.

Having shown that heterogeneous ET in the weak coupling limit is governed by a temperature dependence of the charge transfer rate, we now turn to a discussion of the strong coupling limit. For homogeneous ET, the donor and acceptor potentials (black curves in figure 3(b)) split in the crossing point region (1) so that ET proceeds adiabatically and thermally activated when considering a fully equilibrated electron in the donor potential minimum [10]. The degree of level splitting is determined by the coupling strength, i.e. by the transfer matrix element V_{DA} . In the case of *heterogeneous* ET, the continuum of accepting metal states (orange area) has to be considered again. The grey curves in figure 3(b) depict one of those metal states exemplarily and the resulting level splitting in the crossing point region (2). As $V_{DA} = V_{DA}(E)$, the degree of level splitting may differ with energy. Considering the transfer of an excess electron equilibrated with its surroundings, i.e. in the ground state donor potential minimum, ET is thermally activated. However, in the case of photoinjected electrons, the system relaxes towards the potential energy minimum through solvation (green arrow in figure 3(b)) and therefore passes the continuum of metal states and the corresponding crossing points. As the coupling is strong, charge transfer (red arrow) is very probable and competes with solvation. The ET rate is determined by the large V_{DA} or, to be more precise, by the tunnelling probability along the real space coordinate z (cf figure 1(b)), which results from the wavefunction overlap of the electron with the metal. In this regime, the interfacial ET is temperature-independent. Thermal fluctuations of the solvent play a negligible role for the ET and the charge transfer process in the strong coupling regime can be described by a horizontal evolution in the 2D potential of figure 1.

Actually figure 1(a) indicates schematically both regimes of interfacial ET: in the strong coupling limit discussed above, electron transfer occurs mainly along the electron coordinate z . Due to strong wavefunction overlap with metal states, ET without thermal activation is considerably more probable than ET mediated by thermal activation. The coupling strength (rather than nuclear rearrangement) limits the charge transfer rate. In the weak-coupling limit (yellow to red arrows), the transfer matrix element is sufficiently small to enable thermally activated rearrangement of the solvent molecules (change of solvent coordinate q) enhancing the transfer rate. Fluctuations of the solvent to smaller q (closer to q_A) become more probable with increasing temperature, leading to larger transfer rates for higher temperatures. Thermal

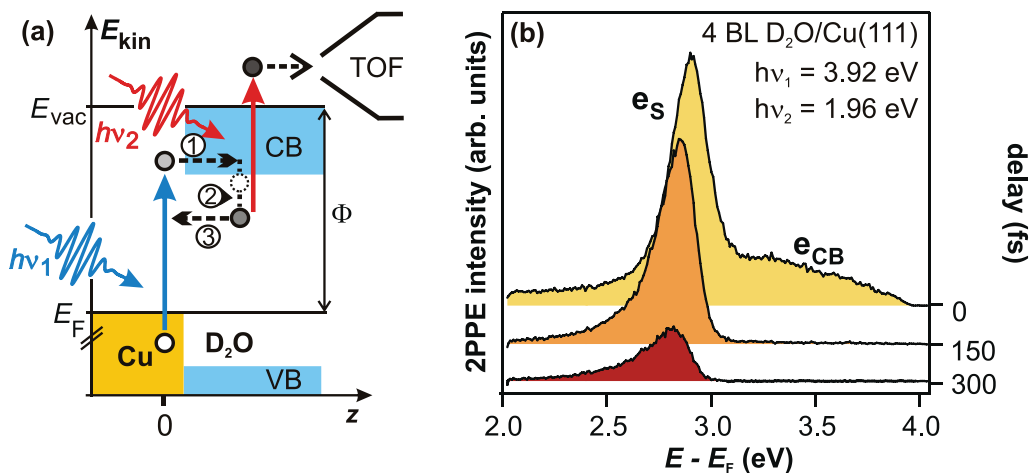


Figure 4. (a) The 2PPE spectroscopy and electron localization and solvation dynamics at the ice–metal interface. (b) Exemplary 2PPE spectra of 4 BL amorphous $D_2O/Cu(111)$ for different time delays.

activation becomes the rate-limiting step for ET. However, it is difficult to draw a distinct line between the strong- and the weak-coupling limit for electron solvation at the polar adsorbate–metal interfaces, as the wavefunction constriction and therefore, the coupling of the excess electrons changes upon solvation. We consider strong and weak coupling as limiting cases of a unifying concept of interfacial ET. The present paper, therefore, uses the term *strongly coupled* for ET dominated by the electronic coupling of the solvated electron to the metal states and *not* affected by temperature variations. The weak-coupling limit is reached when thermally assisted tunnelling, i.e. solvent rearrangement along q , determines the transfer rate.

3. Experimental: time-resolved 2PPE spectroscopy

Time-resolved 2PPE spectroscopy provides a valuable tool to investigate ultrafast electron dynamics at surfaces and interfaces [26, 27]. In the past decade, the surface and image potential states have been used as model systems for 2PPE and theoretical studies, leading to a profound understanding of electronic scattering and relaxation processes at bare metal surfaces [11]. Furthermore, 2PPE spectroscopy has been used to gain insight into ET processes at rare gas–metal interfaces [28]–[30] and solvation dynamics of photoinjected electron in polar adsorbate layers [21], [31]–[33].

In 2PPE, electrons are excited by an ultrashort laser pulse (with photon energy $h\nu_1$) from below the Fermi level E_F to bound intermediate states below the vacuum level E_{vac} , where they may subsequently relax to energetically lower lying states. These electrons are excited by a second, time-delayed laser pulse ($h\nu_2$) to the continuum of final states. Figure 4(a) illustrates the process for photoexcitation and solvation dynamics at the $D_2O/Cu(111)$ interface. The dynamics can be separated into three steps [22]. (i) Photoexcitation from the metal substrate into the conduction band of the ice layer (note that $h\nu_1$ is much smaller than the bandgap of ice and cannot excite electrons inside the D_2O adlayer). (ii) Localization in pre-existing solvation sites and energetic stabilization by molecular reorganization of the polar environment. (iii) Decay of the solvated electron population by ET back to unoccupied states of the metal substrate. As

shown previously, these dynamics can be viewed as a competition between the charge transfer and solvation [23].

Our experimental set-up combines an ultrahigh vacuum (UHV) chamber (base pressure $<10^{-10}$ mbar) for sample preparation and photoelectron spectroscopy with a tuneable femtosecond laser system (for details see [34]). The photoelectron kinetic energy E_{kin} is analysed by a time-of-flight (TOF) spectrometer and the intermediate state energy is determined as $E - E_{\text{F}} = E_{\text{kin}} + \Phi - h\nu_2$, where $h\nu_2$ is the probing photon energy and Φ , the sample work function⁵. Amorphous D_2O films are grown at 100 K on Cu(111) or Ru(001) single crystal surfaces, cleaned by standard procedures [23]. Exemplary 2PPE spectra of 4 BL amorphous $\text{D}_2\text{O}/\text{Cu}(111)$ are depicted in figure 4(b) and exhibit a pronounced peak e_{S} , which is attributed to solvated electrons, and a broad feature e_{CB} , which is resulting from photoinjected electrons in the ice conduction band [19, 22]. After a rapid decay of e_{CB} within the laser pulse duration, the binding energy of the solvated electrons increases (peak shift of e_{S}) due to screening and stabilization of the excess charge within the ice.

4. ET and solvation dynamics at the $\text{D}_2\text{O}/\text{metal}$ interface

In the following, we discuss the influence of temperature on the ultrafast dynamics of ET at amorphous $\text{D}_2\text{O}/\text{metal}$ interfaces. As outlined in section 2, the temperature dependence of the ET rate offers information about the coupling strength of the solvated electron to the metal states. In the case of weak electronic coupling of a photoinjected excess electron, the rate of ET is temperature-dependent due to the reduced nuclear barrier and varying coupling matrix elements V_{DA} (see figure 3(a)). In the strong coupling limit, ET of a photoexcited hot electron to the continuum of accepting metal states is difficult to describe by the Marcus potentials alone (cf figure 3(b)), as charge transfer is dominated by the wavefunction overlap of the electron with the metal [11]. ET occurs solely along the real space coordinate z (figure 1, blue arrow). No temperature dependence of the transfer rate is expected in this regime of charge transfer, as ET due to the large wavefunction overlap is much more probable than transfer mediated by thermal fluctuations of the solvent.

Temperature-dependent 2PPE measurements were performed for the $\text{D}_2\text{O}/\text{Cu}(111)$ and $\text{D}_2\text{O}/\text{Ru}(001)$ systems to determine the regime of electronic coupling, strong or weak, for ET at ice–metal interfaces. Figure 5 depicts the temporal evolution of the 2PPE intensity of the solvated electron state e_{S} for D_2O layers adsorbed on the Cu(111) (blue and green) and on the Ru(001) surface (yellow and orange) for different sample temperatures. The electrons decay considerably faster to the Ru(001) substrate. This effect results from the different surface electronic band structures of Ru(001) and Cu(111) as shown in a previous publication [23]. However, for both datasets, no temperature dependence of the ET rate back to the metal is observed within the first half picosecond and the investigated temperature range (25–91 K for Cu(111) and 99–119 K and Ru(001), respectively). Thus, it can be concluded that the ET at the investigated ice–metal interfaces is *not* thermally activated within the first 500 fs after photoinjection despite the localized character of the solvated charge [19].

The inset of figure 5 depicts the peak shift of the solvated electron distribution at the $\text{D}_2\text{O}/\text{Cu}(111)$ interface as a function of pump–probe time delay. The peak maximum

⁵ The kinetic energy E_{kin} is routinely corrected for the contact potential differences of sample and spectrometer.

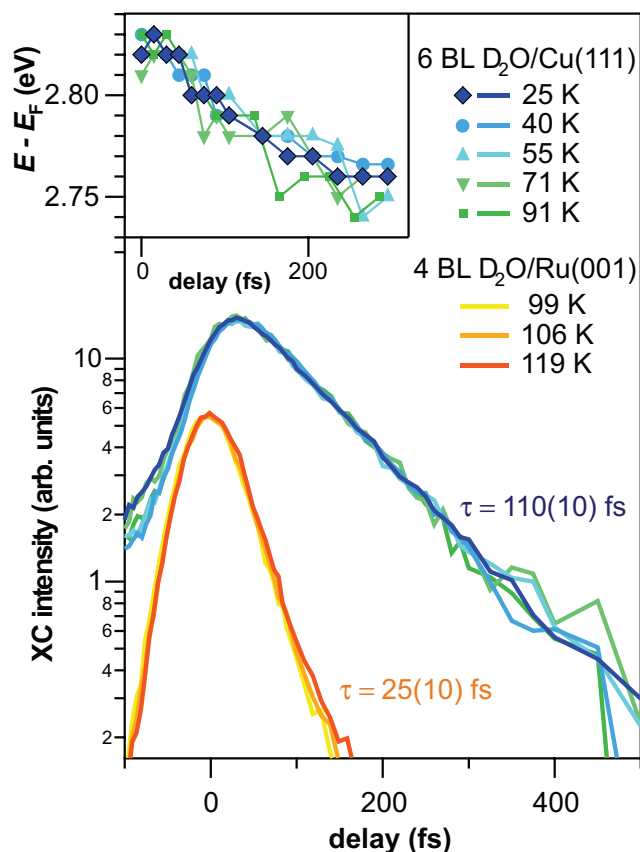


Figure 5. Temperature dependence of ET dynamics for D₂O/Cu(111) and Ru(001). Main panel: population dynamics of solvated electrons at amorphous ice–metal interfaces. The decay is independent of temperature between 25 and 119 K. Inset: shift of the e_s maximum as a function of time delay for D₂O/Cu(111). No temperature dependence is observed.

shifts with $\sim 200 \text{ meV ps}^{-1}$ towards the Fermi level, i.e. the binding energy of the solvated electrons increases. This energetic stabilization of the excess electrons results from the progression of the system along the solvation coordinate q towards the minimum of the donor potential V_D in figure 1. As apparent from the inset in figure 5, this electron solvation is temperature-independent, similar to the electron decay (transfer). It is concluded that thermal activation of reorientations of the solvent molecules is not required in these early stages of solvation. Apparently, the electric field of the excess charge is the driving force for molecular reorientations and thermally induced fluctuations play a negligible role for stabilization. For further details on the dynamical peak shift see [23].

The temperature independence of both population decay *and* energetic stabilization, shows that the initial electron dynamics (delay < 0.5 ps) at amorphous ice–metal interfaces (i.e. immediately after photoinjection) are mediated by strong electronic coupling: (i) screening of the excess charge is not affected by temperature and the corresponding molecular rearrangement and is driven by the electric field of the localized electron. This shows that the D₂O–electron complex has not reached the potential minimum yet. (ii) In addition, ET back to the Cu(111) and Ru(001) substrates is not mediated by thermal fluctuations of the solvent. As shown in

section 2, this means that the coupling between the solvated electron state and metal states is so strong, that direct transfer (for fixed solvent configuration) is considerably more probable than thermally activated tunnelling. The electron population of the solvated electron state decays on fs-timescales, so that only vibrational modes with $\nu > (0.5 \text{ ps})^{-1}$ (or $> 8 \text{ meV}$) can contribute to solvent-driven ET of electrons in $\text{D}_2\text{O}/\text{Cu}(111)$. However, measurements are performed between 25 and 91 K (i.e. 2–8 meV) so that thermal activation should be considered. The presented temperature-dependent measurements of the charge transfer times show unambiguously that ET occurs in the strong coupling limit for ice–metal interfaces.

5. Summary and conclusions

The present contribution addresses the role of thermally activated tunnelling in heterogeneous ET at ice–metal interfaces. We show that both the strong and the weak electronic coupling regimes are limiting cases of a unifying picture of ET. Depending on the transfer matrix element (coupling strength of the interfacial electron to the substrate), the charge is either directly transferred along the electron coordinate z or thermally assisted nuclear rearrangement of the solvent molecules (progression along the solvent coordinate q) becomes the rate-limiting step for ET. In the strong coupling limit, the significant wavefunction overlap of the solvated electron with unoccupied metal states leads to temperature-independent charge transfer. However, for weak electronic coupling between a nascent electron (en route to solvation) and the metal substrate, ET depends on temperature, as thermally activated solvent reconfiguration enhances the transfer rate. Time-resolved 2PPE experiments on amorphous multilayers of D_2O on $\text{Cu}(111)$ and $\text{Ru}(001)$ showed that both ET (back to the metal) and solvation are independent of temperature between 25 K and 119 K. Thus, for these examples heterogeneous ET occurs in the strong-coupling limit.

It should be noted that the fast electron decay at ice–metal interfaces actually prohibits observation of ET in the weak-coupling limit: if charge transfer occurred slower after photoexcitation, the solvent molecules would increasingly screen the excess charge and the system would proceed along the solvent coordinate q towards the potential minimum at q_D in figure 1. With ongoing solvation, the screening of the excess electron from the metal would increase, i.e. the coupling strength would decrease and thermally activated tunnelling could be observed. Observation of such a transition to the weak coupling limit of charge transfer could be possible for solvent–solute complexes that exhibit faster screening from the metal substrate than the ice–metal interfaces. If the decoupling from the metal states occurred before the solvated electron population decays, observation of solvent-driven ET should be possible. A promising candidate for such investigations is NH_3 : as will be shown in a future publication [35], excess electrons in amorphous ammonia adlayers survive considerably longer than hydrated electrons in amorphous ice discussed in the present paper.

Acknowledgments

We thank A Nitzan and D Truhlar for very stimulating and valuable discussions. XYZ gratefully acknowledges the support of a Friedrich Wilhelm Bessel award by the Alexander von Humboldt Foundation. This work has been funded by the Deutsche Forschungsgemeinschaft through SPP 1093 and Sfb 450.

References

- [1] Wasielewski M R 1992 *Chem. Rev.* **92** 435
- [2] Morales R, Charon M-H, Kachalova G, Serre L, Medina M, Gómez-Moreno C and Frey M 2000 *EMBO Rep.* **1** 271
- [3] Roth H D 1990 *Topics in Current Chemistry: Photoinduced Electron Transfer I* ed J Mattay (Berlin: Springer) p 1
- [4] Timpe H-J 1990 *Topics in Current Chemistry: Photoinduced Electron Transfer I* ed J Mattay (Berlin: Springer) p 167
- [5] O'Regan B and Grätzel M 1991 *Nature* **353** 737
- [6] Nitzan A and Ratner M A 2003 *Science* **300** 1384
- [7] Zhu X-Y 2004 *J. Phys. Chem. B* **108** 8778
- [8] Zhu X-Y 1994 *Annu. Rev. Phys. Chem.* **45** 113
- [9] Frischkorn C and Wolf M 2006 *Chem. Rev.* **106** 4207
- [10] Miller R J D, McLendon G L, Nozik A J, Schmickler W and Willig F 1995 *Surface Electron-Transfer Processes* (New York: VCH)
- [11] Echenique P M, Berndt R, Chulkov E V, Fauster T, Goldmann A and Höfer U 2004 *Surf. Sci. Rep.* **52** 219
- [12] Gadzuk J W 1995 *Surf. Sci.* **342** 345
- [13] Marcus R A 1956 *J. Chem. Phys.* **24** 966
- [14] Marcus R A 1957 *J. Chem. Phys.* **26** 867
- [15] Marcus R A 1957 *J. Chem. Phys.* **26** 872
- [16] Nitzan A 2001 *Annu. Rev. Phys. Chem.* **52** 681
- [17] Ge N-H, Wong C M and Harris C B 2000 *Acc. Chem. Res.* **33** 111
- [18] Schenter G K, Garrett B C and Truhlar D G 2001 *J. Phys. Chem. B* **105** 9672
- [19] Bovensiepen U, Gahl C and Wolf M 2003 *J. Phys. Chem. B* **107** 8706
- [20] Miller A D, Bezel I, Gaffney K J, Garret-Roe S, Liu S H, Szymanski P and Harris C B 2002 *Science* **297** 1163
- [21] Zhao J, Li B, Onda K, Feng M and Petek H 2006 *Chem. Rev.* **106** 4402
- [22] Gahl C, Bovensiepen U, Frischkorn C and Wolf M 2002 *Phys. Rev. Lett.* **89** 107402
- [23] Stähler J, Gahl C, Bovensiepen U and Wolf M 2006 *J. Phys. Chem. B* **110** 9637
- [24] Marcus R A 1964 *Annu. Rev. Phys. Chem.* **15** 155
- [25] Marcus R A 1960 *Faraday Discuss.* **29** 21
- [26] Petek H and Ogawa S 1997 *Prog. Surf. Sci.* **56** 239
- [27] Weinelt M 2002 *J. Phys.: Condens. Matter* **14** R1099
- [28] Harris C B, Ge N H, Lingle R L, McNeill J D and Wong C M 1997 *Annu. Rev. Phys. Chem.* **48** 711
- [29] Marinica D C, Ramseyer C, Borisov A G, Teillet-Billy D, Gauyacq J P, Berthold W, Feulner P and Höfer U 2002 *Phys. Rev. Lett.* **89** 046802
- [30] Rohleder M, Berthold W, Güdde J and Höfer U 2005 *Phys. Rev. Lett.* **94** 017401
- [31] Szymanski P, Garrett-Roe S and Harris C B 2005 *Prog. Surf. Sci.* **78** 1
- [32] Bovensiepen U 2005 *Prog. Surf. Sci.* **78** 87
- [33] Li B, Zhao J, Onda K, Jordan K D, Yang J and Petek H 2006 *Science* **311** 1436
- [34] Kirchmann P S, Loukakos P A, Bovensiepen U and Wolf M 2005 *New J. Phys.* **7** 113
- [35] Stähler J, Meyer M, Kusmierik D O, Bovensiepen U and Wolf M 2007 in preparation